We are IntechOpen,
the world's leading publisher of
Open Access books
Built by scientists, for scientists

6,900
Open access books available

186,000
International authors and editors

200M
Downloads

154
Countries delivered to

Our authors are among the

TOP 1%
most cited scientists

12.2%
Contributors from top 500 universities

CLARIVATE ANALYTICS
BOOK CITATION INDEX
INDEXED

WEB OF SCIENCE™

Selection of our books indexed in the Book Citation Index
in Web of Science™ Core Collection (BKCI)

Interested in publishing with us?
Contact book.department@intechopen.com

Flocculation in Estuaries: Modeling, Laboratory and In-situ Studies

Claire Chassagne, Zeinab Safar, Zhirui Deng, Qing He and Andrew J. Manning

Abstract

Modelling the flocculation of particles in a natural environment like an estuary is a challenging task owing to the complex particle-particle and particle-hydrodynamic interactions involved. In this chapter a summary is given of recent laboratory and in-situ studies regarding flocculation. A flocculation model is presented and the way to implement it in an existing sediment transport model is discussed. The model ought to be parametrized, which can be done by performing laboratory experiments which are reviewed. It is found, both from laboratory and in-situ studies, that flocculation between mineral sediment and organic matter is the dominant form of flocculation in estuarine systems. Mineral sediment in the water column is < 20 µm in size and its settling velocity is in the range [0–0.5] mm/s. Flocs can then be categorized in two types: flocs of size [20–200] µm and flocs of size > 200 µm. The origin of these two types is discussed. The two types of flocs are found at different positions in the water column and both have settling velocities in the range [0.5–10] mm/s.

Keywords: Mud, flocculation, sediment transport, population balance equation, Rhine ROFI, Yangtse, floc, aggregation, LISST, monitoring, logistic growth

1. Introduction

Numerical fine sediment transport models make use of hydrodynamic models to estimate the transport (advection and diffusion) of suspended matter in the water column. In most numerical models, a few classes of suspended matter are defined. Each class is defined as a collection of particles having the same (often time-invariant) settling velocity and a concentration of suspended matter per class (suspended mass per unit of volume). The models are calibrated using in-situ observations, whereby suspended mass concentrations are measured at given locations in time. The settling velocity chosen for each class is based on in-situ observation of settling velocity and model calibration. To give an order of magnitude, it is generally found that using 3 classes of particles, with settling velocities of the order of ≤0.01 mm/s, 0.1 mm/s and ≥ 1 mm/s enables to correctly predict the Suspended Particulate Matter (SPM) in space and time for a large number of situations in coastal areas [1–5].

In the context of sediment transport modeling, several open questions however remain.

The hypothesis that the classes of particles do not interact is for instance questionable in estuarine regions, where fine particles are known to be in the form of flocs. Several studies over the years have therefore concentrated on implementing flocculation in sediment transport models [6–9]. Flocs are aggregates of mineral sediment particles, most often combined with organic matter. The underlying question, in terms of (numerical) modeling is related to flocculation dynamics. Are the models used at present, based on Population Balance Equations (PBE) adequate to capture the physical processed occurring in-situ? Which alternative equations, representing the flocculation process, should otherwise be implemented in a numerical model? This question will be addressed in Section 2.

Modeling flocculation requires to know the relevant parameters that plays a role in the process. Some of these parameters are for instance salinity, shear stress and type of organic matter present. The influence of each parameter on flocculation can be studied in a systematic way in the laboratory, but how do lab studies relate to in situ measurements? How should these parameters be accounted for in a numerical model? This question is addressed in Section 3.

Settling velocities are difficult to assess in situ [10, 11]. Measurements of the settling velocities of particles in quiescent water can be done by performing on board experiments [12–14]. These experiments consist in carefully pipetting a sample and let particles settle in a column filled with water of same composition as the one at the sample location. The settling velocity of particles in still water is then recorded by video microscopy. From the videos, the size, aspect ratio and Stokes settling velocity of each particle can be estimated.

The disadvantages of this method are: (1) only a limited number of samples can be taken and (2) the structure and velocity of the flocs can be altered through sampling and during settling, due to collective particle effects. Especially point (1) is of concern. As sediment transport models are run over large period of times, the interaction between particles and hydrodynamics are better understood if longer time series of measurements can be performed. The longer time series measurements performed in situ enable to assess particle size distributions (PSD), the volume concentration of suspended particles and suspended sediment (mass) concentration (SSC) based on light scattering (and also acoustic) techniques. Combining these measurements, a rough estimate of the mean settling velocity of particles can be given, using Stokes law [15, 16]. The question is whether this mean settling velocity is in agreement with the on board settling experiments. This question is specifically discussed in Section 3.2. A brief summary and outlook is given in the last section.

2. Flocculation models

Traditionally, flocculation is modeled using population balance equations (PBE), which were introduced in 1917 by Smoluchowski [17–19]. These equations represent the change in concentration of classes of particles over time, whereby a class is defined as a collection of identical particles. Each particle (floc) in class k has the same size L_k, and contains the same number k of primary mineral clay particles. If n_k is the number of class k particles per unit of volume, there are $k \times n_k$ primary particles per unit of volume in class k. The change in time of the number of particles within a class $n_k(t)$ is a function of the collision frequency and the collision efficiency between particles, as well as a function of the break-up of an aggregate, usually due to shear.

PBE models have successfully been applied to model the flocculation of suspensions destabilized by addition of salt [18, 19]. An example is for instance the

aggregation that is likely to occur when fine mineral sediment particles are advected from fresh to saline environment.

In the presence of organic matter, however, the flocculation mechanisms cannot properly be modeled using PBE's for the following reasons:

- the size of a floc is not connected anymore to the number of primary mineral clay particles that composes the floc, since for a same size, a floc could be formed by aggregation of different amounts of organic matter and mineral sediment. Particles can break-up due to shear, but polymeric flocs are elastic and usually tend to coil under shear without breaking. Their shape and size thus can change over time from elongated to spherical without loss of mass.

- the collision frequency in PBE models is a function of the diameter of the colliding particles. Organic particles can have very anisotropic shape, and extracellular polymeric substances (EPS) that are a major driver for flocculation consist of elongated, flexible polymeric chains, composed mainly of polysaccharides, proteins and DNA. Their radius of gyration is a function of shear and water properties (such as salinity). The expression for the collision frequency is in this case unknown.

Some authors have tried to adapt PBE models to mimic the floc size evolution, but doing this implies to add a significant amount of unknown parameters to the model, even for a model accounting for only 3 classes of particles (microflocs, macroflocs and megaflocs) [6]. To parametrize the model, the following adjustable parameters are required (number of parameters in parenthesis): the mass fraction of microflocs produced when a macrofloc or a megafloc breaks up (2); the mass fraction of the remaining megafloc when a larger megafloc breaks up (1); the number of generated microflocs and macroflocs when a larger macrofloc or megafloc breaks up (4); the number of microflocs in one macrofloc or megafloc, or fractal dimension of microflocs and macroflocs (2); the collision efficiency, taken to be constant, but could be class-dependent (1); the collision frequency between microflocs, macroflocs and megaflocs (6); the breakup frequency of a megafloc and a macrofloc (2). These 18 parameters are difficult to estimate and therefore they are used as calibration parameters.

Recently, a simpler approach to model flocculation, that makes use of logistic growth theory, was proposed [20]. Logistic growth models are conveniently used to model systems whereby rate constants can be measured, such as the growth and decay of a bacterial community over time. In the context of flocculation, one can think of increase and decrease of the number of particles within a size class in terms of growth (birth) and decay. The time evolution of the concentration of particles within a class n (we here omit the subscript k for simplicity) is given by:

$$\frac{dn}{dt} = [b(t) - d(t)]n \tag{1}$$

where the birth function $b(t)$ and the decay function $d(t)$ are given by

$$b(t) = \frac{1}{t_b} \cdot \frac{a_b \exp\left(-\frac{t}{t_b}\right)}{1 + a_b \exp\left(-\frac{t}{t_b}\right)} \tag{2}$$

$$d(t) = \frac{1}{t_d} \cdot \frac{a_d \exp\left(-\frac{t}{t_d}\right)}{1 + a_d \exp\left(-\frac{t}{t_d}\right)} \tag{3}$$

There are 4 unknown parameters, a_d, a_b, t_d and t_b for each class of particles. Birth and decay are associated with the characteristic timescales t_b and t_d and a_b and a_d are parameters that influences the flocculation rates, see Eq. (7). The analytical solution of Eq. (1) is given by

$$n(t) = n_\infty \frac{1 + a_d \exp\left(-\frac{t}{t_d}\right)}{1 + a_b \exp\left(-\frac{t}{t_b}\right)} \tag{4}$$

The parameter n_∞ represents the value of $n(t)$ at long times, after the particles might have experienced birth and decay (or only birth or only decay). The flocculation rate dn/dt can be defined as being the slope of $n(t)$ at the onset of aggregation,

$$n(t \to 0) = n(t = 0) + \frac{dn}{dt} \times t \tag{5}$$

with

$$n(t = 0) = \frac{1 + a_d}{1 + a_b} n_\infty \tag{6}$$

$$\frac{dn}{dt} = n_\infty \frac{a_b(1 + a_d)/t_b - a_d(1 + a_b)/t_d}{(1 + a_b)^2} \tag{7}$$

The main advantage of Eqs. (1) and (4) is that each class can be seen as independent of each other: it is possible to estimate the evolution of one class only (for instance the class corresponding to the most abundant type of particles found in the water column). With 4 parameters, it is hence possible to parametrize the flocculation kinetics through Eq. (1) which is the equation required in numerical models, see Section 2.1.

2.1 Classes of particles

In the previous section, a new model was proposed to study the time evolution of a class of particles. As discussed in that section, because of the presence of organic matter, a class of particles cannot be defined as flocs containing the same number of primary particles. This is why, for the model proposed in Section 2.2, two types of particles will be distinguished: "primary" particles (Class 1) which are unflocculated mineral sediment particles and "flocs" (Class 2), which are particles aggregated with an unspecified amount of organic matter. The settling velocity of primary particles can be assumed to be a constant, but the settling velocity of flocs is a function of time, as the floc can get denser under the action of shear, or gain in volume and mass by further aggregation.

Class 1: class of particles defined as being mineral sediment particles. The mass concentration of Class 1 in the water column is $m_1(t)$ and the settling velocity associated to this class is $w_{s,1}$ which is assumed to be constant. The total clay mass in Class 1 per unit of volume is given by $m_1(t) = V_1(t) \times \rho_p$ where V_1 is the total volume occupied by Class 1 particle per unit of volume and ρ_p the absolute density of clay particles, which is of the order of 2600 kg/m³. The total volume of particles in Class 1 per unit of volume is given by $V_1 = n_1(t) \times V_p$ where V_p is the volume of a particle in Class 1. In case that Class 1 is composed of polydisperse particles, one can subdivide Class 1 in different fractions based on size: $V_1 = \sum n_{1,i}(t) \times V_{p,i}$

where each particle in sub-class i has a volume $V_{p,i}$. The volumes V_1 and V_p can be estimated from in-situ particle size measurements, see Section 3.

Class 2: class of particles defined as flocs. The mass $m_2(t)$ represents the mineral clay mass (not the floc mass) per unit volume contained in Class 2. The settling velocity associated to flocs in this class is $w_{s,2}(t)$ which is assumed to be time-dependent. We will see, from in-situ measurements, that Class 2 can be split in two (Class 2a and Class 2b). Class 2b flocs have a smaller density and larger size than Class 2a flocs but a comparable settling velocity range.

Two types of flocculation are distinguished:

Microflocculation: this process describes the capture of primary particles by suspended organic matter or by existing flocs. This implies a transfer of mineral sediment mass between Class 1 and Class 2. A primary particle that is captured will experience a change in settling velocity, and be transported differently. A small colloidal mineral particle can be transported over larger distances than the same particle when it is imbedded in a floc. The sources and sink terms of mineral clay in the water column are located at the boundaries of the domain: mineral clay can be advected from the rivers into the sea or re-suspended from the bed due to shear. The resuspension of unflocculated mineral sediment from the bed occurs:

- during storm or dredging periods, when the fluff layer (containing organic matter) that constitutes the top of the sediment bed has been eroded.

- when the organic matter has decayed sufficiently to release primary particles from the bed. This happens mainly during the winter season.

Macroflocculation: this process describes the capture of a floc by another floc. There is no mass transfer between classes as all particles experiencing macroflocculation remain in Class 2. We will see that this process, even though occurring in the water column, is most probably not the dominant one in terms of sediment transport. When two flocs aggregate, their settling velocity will change. However, we will show that there is a large spread in settling velocity for flocs, even without flocculation, as the settling velocity changes due to coiling under shear. For numerical modeling purposes, it is therefore not necessary to account for macroflocculation, as no clear correlation can be made, at this stage, between macroflocculation and change in settling velocity.

Flocculation, in terms of numerical modeling, is hence defined as the mineral sediment mass transfer between Class 1 and Class 2. All the primary particles which leave Class 1 by flocculation become part of Class 2. Flocs that aggregate or break in smaller flocs remain part of Class 2. The transfer from Class 2 to Class 1 occur when organic matter in flocs has decayed sufficiently to free mineral particles.

2.2 Inclusion of flocculation in a sediment transport model

The inclusion of flocculation in a sediment transport model is done by expressing the advection–diffusion equations for the two mass classes of particles. The equations presented below are for the special case where only vertical advection and diffusion is considered. Generalization to other coordinates is straightforward.

Step 1 At the first numerical step, particles are entering or leaving a volume element by advection/diffusion:

$$\frac{\partial m_1}{\partial t} + \frac{\partial((v_z - w_{s,1})m_1)}{\partial z} - \frac{\partial}{\partial z}\left(D_z \frac{\partial m_1}{\partial z}\right) = 0 \tag{8}$$

$$\frac{\partial m_2}{\partial t} + \frac{\partial((v_z - w_{s,2})m_2)}{\partial z} - \frac{\partial}{\partial z}\left(D_z \frac{\partial m_2}{\partial z}\right) = 0 \tag{9}$$

The parameters v_z and D_z represent the vertical water velocity and eddy diffusion and w_s represents the vertical settling velocity of a particle under the influence of gravity. The new mass concentrations $m_1(t + dt/2)$ and $m_2(t + dt/2)$ are obtained.

Step 2 At the second numerical step, flocculation occurs within the volume element, and a mass transfer occurs between Class 1 and 2:

$$\frac{\partial m_2}{\partial t} = -\frac{\partial m_1}{\partial t} \tag{10}$$

The mass transfer can be modeled by equations similar to Eq. (1). In the simple case where only aggregation (no break-up) occurs, one gets

$$\frac{\partial m_1}{\partial t} = -d_1(t) \times m_1 \tag{11}$$

$$\frac{\partial m_2}{\partial t} = b_2(t) \times m_2 \tag{12}$$

And it follows from Eq. (10) that $d_1(t) \times m_1 = b_2(t) \times m_2$. Both birth and decay functions are function of the mass of organic matter present in the water. The new mass concentrations $m_1(t + dt)$ and $m_2(t + dt)$ are obtained. The dynamics of the mass transfer between Class 1 and Class 2 are discussed in Section 3.

The average settling velocity of Class 1 particles is given by

$$w_{s,1} = \frac{d_p^2}{18\eta}\left(\rho_p - \rho_w\right)g \tag{13}$$

This velocity is a constant as function of time. The average size of primary particles can be assessed by Laser In-Situ Scattering and Transmissometry (LISST) data in-situ or laboratory PSD measurements from samples collected in-situ. Settling column experiments combined with video microscopy can confirm the values estimated for $w_{s,1}$.

Step 3 At the third numerical step, the change in settling velocity of Class 2 particles is addressed. The link between particle number, mass and volume concentration is not straightforward for Class 2 particles. Class 2 particles evolve in time, as flocs can aggregate, break or coil, hereby changing their size, aspect ratio and density, and therefore their settling velocity – a key parameter for numerical modeling. The settling velocity of Class 2 particles is given by

$$w_{s,2}(t) = \frac{[d_f(t)]^2}{18\eta}\left(\rho_f(t) - \rho_w\right)g \tag{14}$$

Whereby both the average size of flocs d_f and its density ρ_f should be updated as function of time. In Section 2.3 we describe how $w_{s,2}$ can be estimated from in-situ measurements and in Section 2.4 how analytical functions can be obtained from laboratory experiments.

Boundary condition The boundary condition at the fluid/bed interface can be written in terms of mass fluxes. One flux is the mass flux settling down to the bed and given by $w_{s,k}m_k$. The other is the erosion flux, which is usually written in the form $M_k(\tau/\tau_c - 1)$ where M_k is mass per unit of area and time that leaves the bed, τ is the bottom shear stress and τ_c is the stress at which the bed start to be eroded.

If the bed is composed of a fluff layer with underneath a organic matter-degraded bed, it is assumed that the erosion will be different for each layer. The mass transfer from Class 2 to Class 1 inside the bed by degradation of organic matter is given by an equation analogous to Eq. (10). The parametrization of this equation is an ongoing topic of research.

2.3 Estimation of the settling velocity from in-situ measurements

To estimate the mean density of the flocs ρ_f, one assumed it is given by

$$\rho_f = \frac{m_f + m_w}{V_f} \tag{15}$$

where m_f (g) is the mass mineral sediment inside a floc and m_w (g) the mass water inside a floc (it is therefore assumed that the density of organic matter is close to the one of water) and V_f (L) is the volume of a floc. It follows that

$$\rho_f - \rho_w = \left(1 - \frac{\rho_w}{\rho_p}\right)\frac{m_f}{V_f} \tag{16}$$

where ρ_f is the floc density (g/L), ρ_w is the ambient water density (about 1000 g/L), ρ_p is the sediment absolute density (usually taken to be equal to the mineral sediment density, i.e. of the order of 2650 g/L). Realizing that

$$\frac{n_2 m_f}{n_2 V_f} = \frac{m_2}{V_2} \tag{17}$$

where V_2 (L/L) is the volume occupied by Class 2 flocs per unit of volume and assuming that $V_2 \gg V_1$ (where V_1 is the volume occupied by Class 1 particles per unit of volume) one gets

$$\rho_f - \rho_w = \left(1 - \frac{\rho_w}{\rho_p}\right)\frac{m_2}{V_{tot}} \tag{18}$$

where V_{tot} (L/L) is the total volume of particles detected per unit of volume. It represents the volume occupied by the sediment in a given volume of water and can be measured in-situ by LISST, which also provides full PSD's (in the range 2–500 μm) as function of time. The mean floc size d_f can therefore also be estimated from LISST data.

We recall that m_2(g/L) represents the total mass of mineral clay per unit volume inside Class 2. Note that most authors assume that $m_2 = m_{clay}$ (the total mass of mineral clay in suspension) hereby implying that there are no Class 1 particles in suspension. This approximation can lead to an overestimation of the floc density since despite representing a small volume of the total volume compared to Class 2, Class 1 particles may represent a non-negligible part of the total sediment mass. The mass m_{clay} is the mass suspended mineral sediment per unit of volume (g/L) also denoted SSC (suspended sediment concentration) and usually estimated in-situ by Optical Back Scattering (OBS) technique.

From the estimation of $\left(\rho_f - \rho_w\right)$ and d_f the settling velocity $w_{s,2}(t)$ can be evaluated.

2.4 Estimation of the settling velocity from models

Considering the fact that a lot of data has been collected over the years to link the mean floc size to parameters such as shear rate and salinity, the time evolution of the mean floc size d_f can be parametrized as function of these variables [21–25]. It has been shown for example that in the case of salt-induced flocculation the equilibrium floc size is given by

$$d_{f,eq} = CG^{-\gamma} \tag{19}$$

Where C and γ are constants to be fitted. Values γ are around [0.29–0.81] whereas for C they are in the range $[10^{-3} - 10^{-2}]$ m/s$^{1/2}$ [22]. As shown in Section 3.1.1, salt-induced grown flocs will never exceed the Kolmogorov microscale d_K given by

$$d_K = \left(\frac{G}{\nu}\right)^{-0.5} \tag{20}$$

Where ν is the kinematic viscosity which is of the order of 10^{-6} m^{2}s^{-1} for water at 20°C. From laboratory experiments, the time evolution of the mean particle size can be modeled using the same type of logistic growth model as presented in Eq. (4):

$$d_f(t) = d_{f,eq} \frac{1 + a_{f,d} \exp\left(-\frac{t}{t_{f,d}}\right)}{1 + a_{f,b} \exp\left(-\frac{t}{t_{f,b}}\right)} \tag{21}$$

where the parameters $d_{f,eq}$, $a_{f,d}$, $a_{f,b}$, $t_{f,d}$ and $t_{f,b}$ are found by fitting experimental results. By performing a large number of laboratory experiments, where each of the relevant parameters (salinity, organic matter, shear) can be varied independently of one another the dependence of $d_{f,eq}$, $a_{f,d}$, $a_{f,b}$, $t_{f,d}$ and $t_{f,b}$ on these parameters can be found. This work is currently going on [20]. The floc density is found from settling velocity measurements, and is usually parametrized using the relation

$$\rho_f - \rho_w = \left(\rho_p - \rho_w\right)\left(\frac{d_f}{d_p}\right)^{D-3} \tag{22}$$

where D is a parameter (often designated as "fractal dimension") between 1.5 and 3 and d_p a characteristic size, such that $d_p \leq d_f$. A large amount of data is available for the parameters D and d_p, but a systematic study of their dependence on the relevant parameters is still missing.

From Eqs. (14), (20) and (21) the settling velocity $w_{s,2}(t)$ can be evaluated.

3. Laboratory studies and in-situ monitoring

3.1 Laboratory studies

Laboratory experiments have the great advantage that the sample under investigation is in a closed volume, and that therefore the mineral clay mass is conserved during the experiment. This enables to estimate mass balances that are required for flocculation models.

3.1.1 Flocculation by salt and pH

In **Figure 1**, some examples are given of the mean particle size evolution for different salinities and pH. At low pH, the edges of the clay particles are positively charged, leading to Coulombic attraction between the negatively charged faces and the positively charged edges. Flocs will be created whereby the particles preferably arrange themselves in a so-called house of card structure. At pH > 7, clay particles are overall negatively charged and flocculation is driven by van der Waals attraction, when the Coulombic repulsion has been screened by sufficient addition of salt [25]. The main features of these type of flocculation mechanism are:

- the time to reach a steady-state mean floc size is of the order of hours

- the flocs produced are always smaller than the Kolmogorov microscale

As discussed in the previous section, this type of flocculation will not be the preferred mode of aggregation in estuarine systems. Flocs in these systems will in majority contain some proportion of organic matter. Organic matter-induced flocculation is very fast, especially in saline environment, where Coulombic repulsion between particles of same charge is neutralized.

3.1.2 Flocculation by organic matter

An example is given here of polymer-induced flocculation. For this example 0.7 g/L of river clay with 4.7 mg/L polymeric cationic flocculant was used. Typical example of cationic flocculant in the water column are polysaccharides. The flocculant to clay ratio is 6 mg/g. The optimal flocculant dose is defined as the flocculant to clay ratio which leads the fastest to the creation of large flocs. The optimal dose for flocculation with this cationic flocculant for the studied clay was found to be around 5 mg/g flocculant to clay ratio [26]. Another example can be found in [20], where a ratio of 0.71 mg/g was used (lower than optimal dose).

The composition of the clay used is predominantly quartz, calcite, anorthite and muscovite [27]. The flocculant, referenced ZETAG 7587, is composed of a copolymer of acrylamide and quaternary cationic monomer usually used for the conditioning of municipal and industrial substrates.
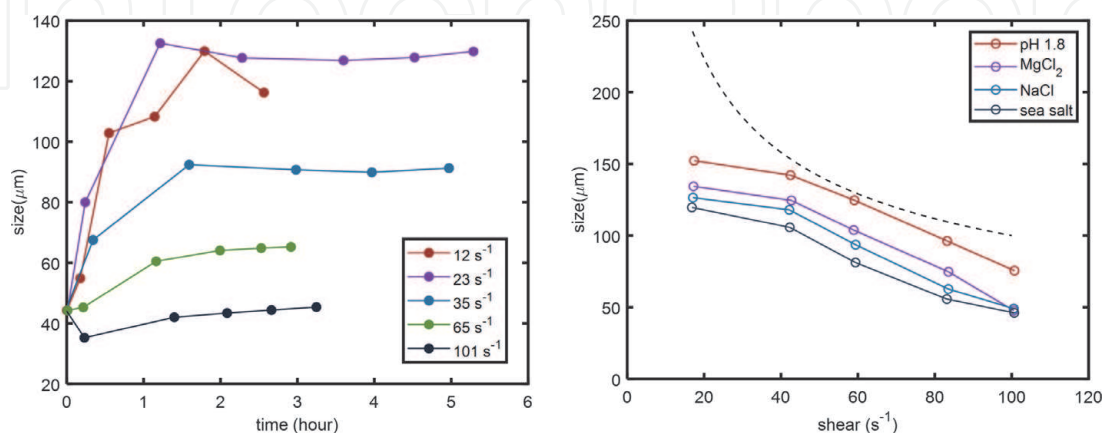

Figure 1.
Left panel: Time evolution of the mean particle of a kaolinite suspension (0.135 g/L) at pH = 9.3 with 100 mM of added $MgCl_2$ for different shear rates. Right panel: Mean particle size at steady-state as function of shear rate. Mud was taken from the lower Western Scheldt (0.135 g/L). The sample at pH = 1.8 has no added salt, the other samples were at pH = 8. The salts used (indicated in the legend) were: $MgCl_2$ (40 mM), NaCl (100 mM). The dashed line corresponds to the Kolmogorov microscale. Data is adapted from [18].

The particle size distribution (PSD) and mean particle size (D50) as function of time of this suspension was measured by static light scattering using a Malvern MasterSizer 2000, with a procedure described in [20, 27]. The PSD of the clay sample is given as the PSD at t = 0 s. At a time defined as t = 1 s flocculant was added to the clay suspension. The Particle Size Distributions (PSD) are given following the class distributions of the software of the static light scattering device. The size distribution is given by

$$d_k(\mu m) = 10^{0.05 \times k}/50 \qquad (23)$$

where k is an integer number between 1 and 100 and represents the number of the class associated to a given size (diameter) d_k. For instance, k = 46 corresponds to particle d_{46} = 4 μm and k = 84 corresponds to particle size d_{84} = 320 μm. A hundred size bins are so created. In the experiments the concentration of each size class is given in terms of percent volume concentration $V_{k,\%}$ (volume occupied by Class k particles divided by the volume occupied by all particles) and consequently $\sum_{k=1}^{100} V_{k,\%} = 100\%$.

The samples were further analyzed by video microscopy. This was done using a LabSFLOC-2 camera system (Laboratory Spectral Flocculation Characteristics, version 2) which records the settling velocity of particles from a pipetted amount of sample. From the settling velocity, the particle size, shape and density were estimated [28, 29].

The time evolution of the PSD of this suspension is given in **Figure 2**. The flocculation is very fast, as the cationic flocculant concentration is close to the optimal dosage.

One can see that the results obtained by video microscopy are in close agreement with the ones obtained from laser scattering. The % volume of particles below 100 μm is larger by video microscopy than by laser scattering. The PSD peak obtained by laser scattering is wider than the one obtained by video microscopy. It was observed that PSD's obtained from this particle sizer overestimated the largest sizes [27]. Consequently, as the total volume should give 100%, the % volume of smaller particles is underestimated.

Two types of fits were performed: first the data set was fitted considering times below 250 s, and then the same data set was fitted for the duration of the experiment (1835 s). The corresponding time evolution of the different size classes are given in **Figure 3**.

From the analysis of all the size classes, it is clear that some classes are not representative of a flocculation process, like class size 106 μm in **Figure 3**, which is
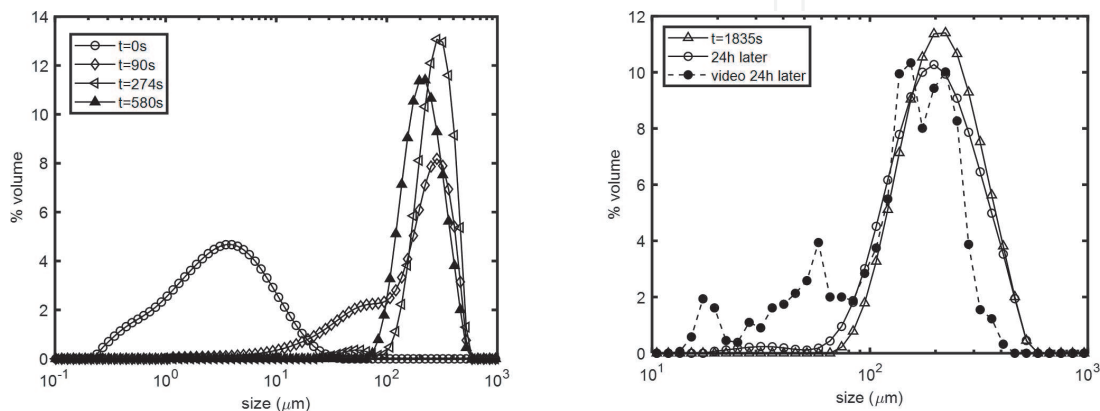

Figure 2.
Time evolution of the PSD of a clay suspension (0.7 g/L) in presence of 4.7 mg/L of cationic flocculant (added at t = 1 s); the video microscopy data has been acquired using the LabsFLOC-2 camera system.
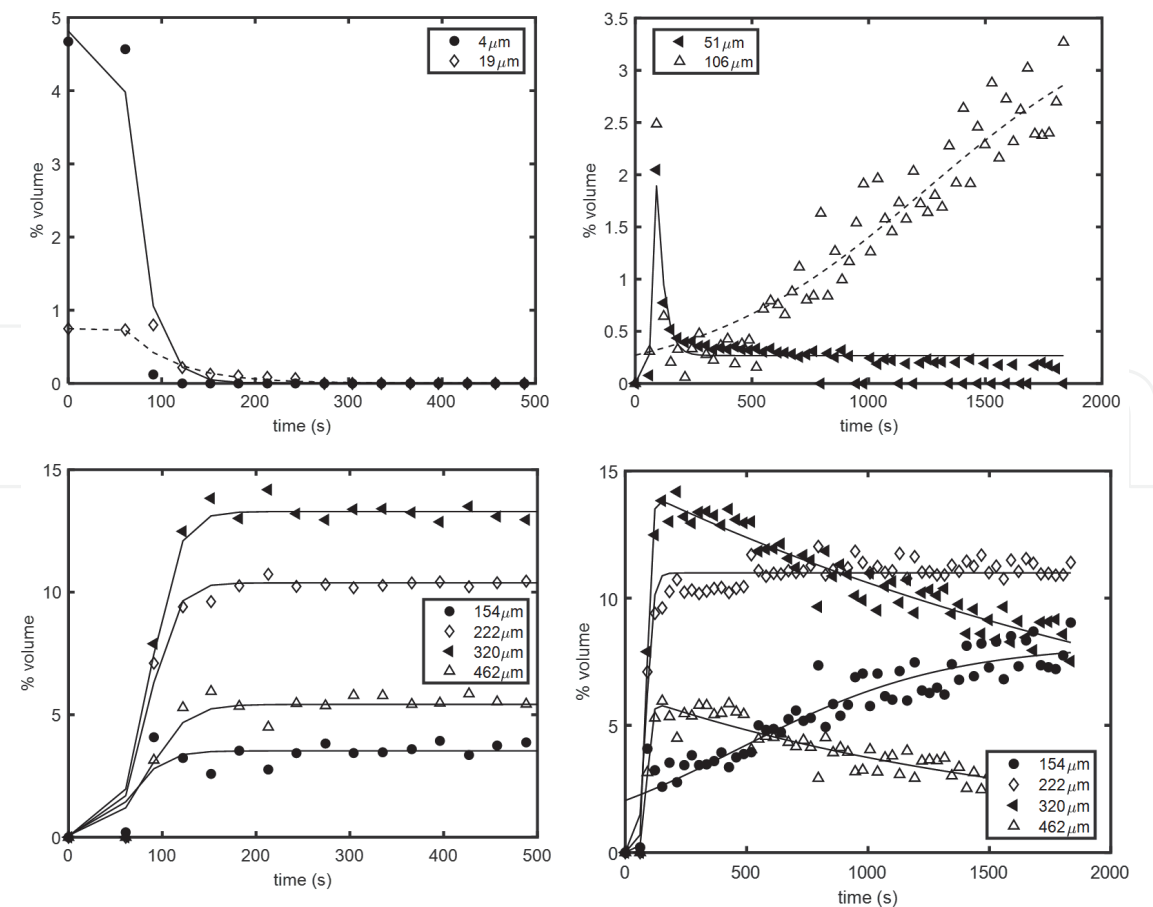
Figure 3.
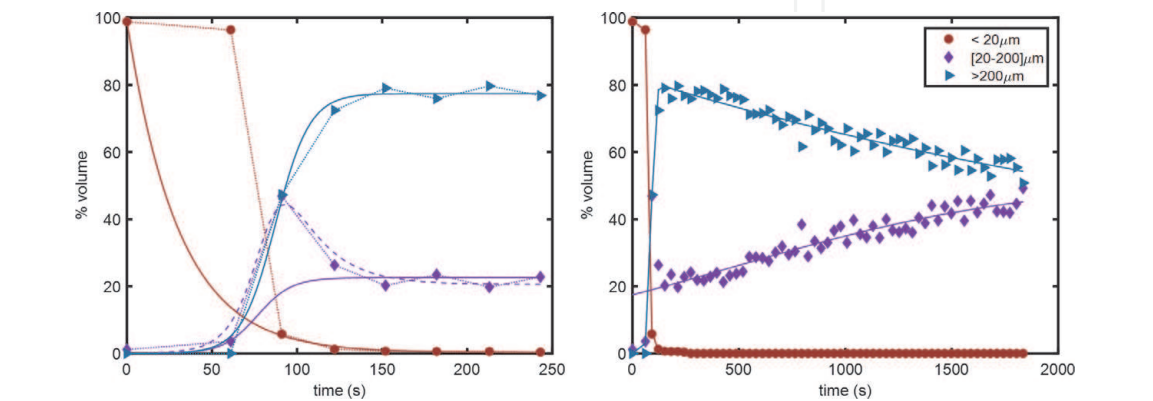*Time evolution of the concentrations of a different size classes (given in the legends); clay suspension (0.7 g/L) in presence of 4.7 mg/L of cationic flocculant (added at t = 1 s). The lines represent fits obtained from the analytical model. Bottom panel, left: Fits for the period [0–500 s]. Bottom panel, right: Fits for the entire duration of the experiment.*

located in-between the high-end tail of the initial clay PSD and the low-end tail of the flocculated clay PSD.

In order to represent the typical behavior of particles under flocculation, it is therefore better to define size classes as wider groups, containing particles in a given size range. From the fits of all classes, three size classes are proposed. Similar classes have been identified by other authors, from in-situ studies [30, 31]. Replotting the data by creating three size classes gives **Figure 4**.

Figure 4.
Time evolution of the concentrations of three size classes (given in the legends); clay suspension (0.7 g/L) in presence of 4.7 mg/L of cationic flocculant (added at t = 1 s). The full and dashed lines represent fits obtained from the analytical model.

The characteristics of the 3 classes are:

Class 1: particles of size <20 μm. These particles represent the unflocculated mineral clay that was present at the onset of the experiments. The concentration of this class goes to zero over time as none of the clay is left unflocculated in this experiment.

Class 2a: particles of size [20–200] μm. These flocs are created at the onset of the experiment. Their concentration increases at longer times.

Class 2b: particles of size >200 μm classes. The flocs are largely created at the onset of the experiment, but their concentration decreases over time, due to coiling.

By analyzing the behavior of the classes, several characteristic times can be identified. The data was fitted for the time period between [0–250] s (**Figure 4**, left panel) and for the whole duration of the experiment (**Figure 4**, right panel). It is shown, by taking Class 2a as an example (left panel, short times fit) that the data can be fitted correctly using the full analytical equation Eq. (4) with birth and decay (dashed line). The choice is made, however to use only a decay function for Class 1 and birth functions for Classes 2a and 2b (full lines), so as to analyze the most important dynamics of these classes at short times. The associated characteristic times and birth and decay rates are given in **Table 1**.

Two behaviors are observed:

- within the first 100 s of the experiment, flocculation (mass transfer between Class 1 and 2) has occurred.

- at longer time (in a matter of hours) there is a significant change in size for Class 2 particles, whereby large flocs (from Class 2b) coil and start to populate size Class 2a.

Twenty-four hours after the start of the experiment, the sample was re-measured after the steering was stopped overnight. The found PSD is given in **Figure 2**, along the PSD found from the analysis of a subsample by video microscopy. From video microscopy 1550 particles were recorded, and their sizes were divided into the same size classes as given by Eq. (23). The volume concentration of particles in each class was thus estimated. The settling velocity and estimated density of the particles from Stokes' law are given in **Figure 5**, along with the aspect ratio of each particle. One can observe that the aspect ratio is quite large for many particles. Most particles with high aspect ratio have been formed by differential settling during the video microscopy experiment, where it was observed that flocs that were touching immediately stuck to each other (a consequence of the fact that the flocculant to clay ratio is close to the optimal dose).

Using again Eq. (23) to create bin sizes, the data is replotted in **Figure 6**, top panel. The classes are furthermore divided in the three size classes 1, 2 and 3 (lower panel).

The density as function of size was estimated using Eq. (22). The characteristic size d_p was taken to be the smallest recorded particle, viz. 13 μm. The density ρ_p was

Class size	Flocculation rate (% s^{-1}) for [0–250] s	Flocculation rate (% s^{-1}) for [0–1835] s
Class 1: < 20 μm	−3.2 (t_d = 70 s)	0
Class 2a: [20–200] μm	0.0011 (t_b = 10 s)	0.018 (t_b = 673 s)
Class 2b: >200 μm	0.0012 (t_b = 10 s)	−0.022 (t_d = 2231 s)

Table 1.
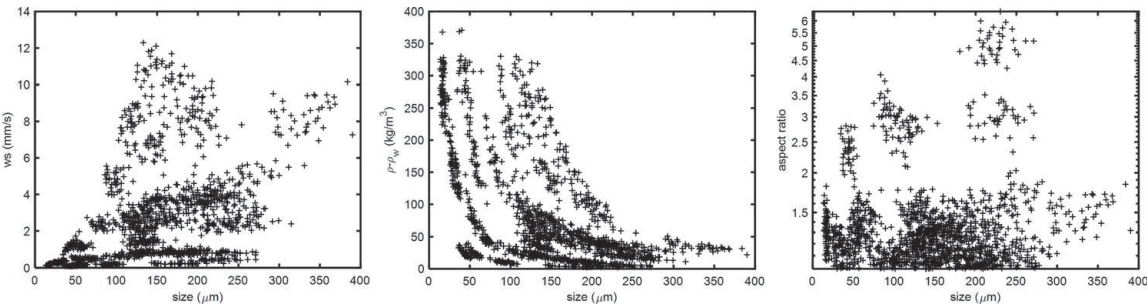*Aggregation kinetics for the three classes. Characteristic times for birth or decay are given in parenthesis.*

Figure 5.
Settling velocity, estimated density (from Stokes' law) and aspect ratio of the sample corresponding to "video 24h later" in **Figure 2**.
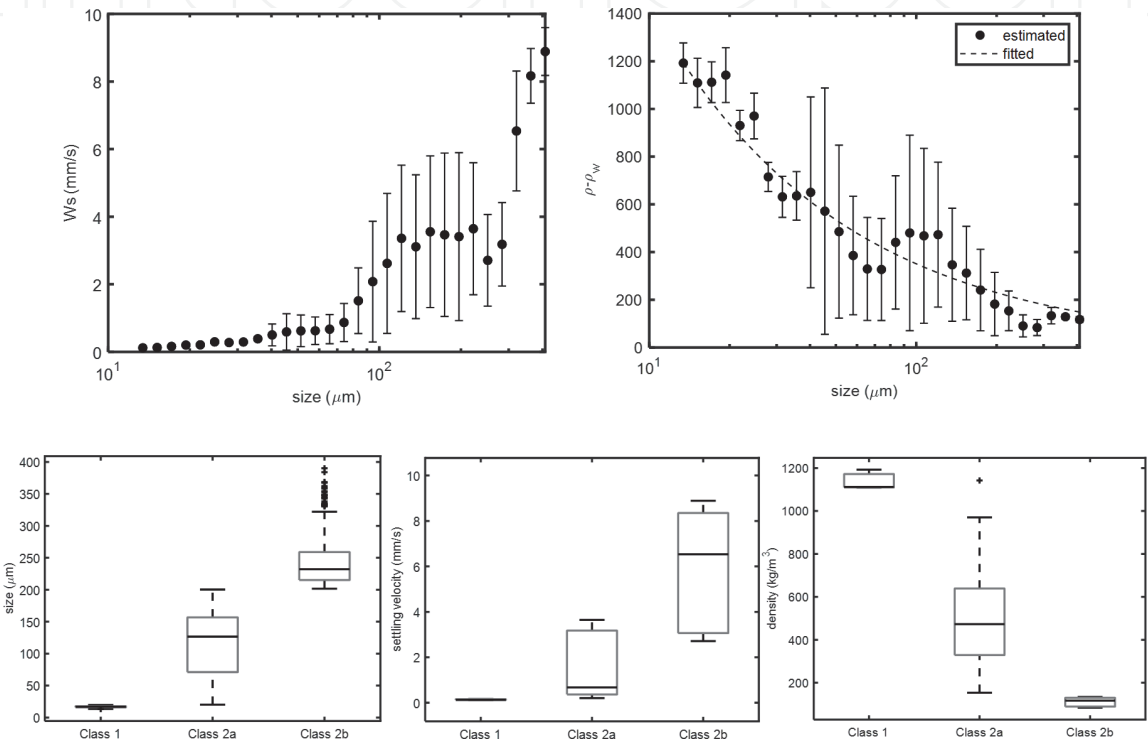

Figure 6.
Settling velocity, estimated density (from Stokes' law) and sizes of the sample corresponding to "video 24h later" in **Figure 2**.

taken to be the average density of the particles of class size 13 μm (2250 kg/m³), ρ_w is the density of water (1000 kg/m³), and D was found to be 2.39. It can be seen that, even if Eq. (22) is a good approximation for the density behavior, there is a large scatter in the measured data, as particles in Class 2a have a relative density that varies between 100 to 1000 kg/m³, resulting in settling velocities ranging between 0.5 and 5 mm/s.

For each PSD measurement using the laser diffraction technique the total volume of particles detected per unit of volume V_{tot} (L/L) is known. At t = 0 all clay is unflocculated and it is therefore easy to estimate the expected V_{tot} from the clay concentration in the jar (m_{clay}) and the absolute density of mineral sediment ρ_p:

$$V_{tot} = \frac{m_{clay}}{\rho_p} = \frac{0.7 \text{ g/L}}{2650 \text{ g/L}} = 0.0265\% \qquad (24)$$

which is very close to the value of 0.0273% found by laser diffraction. In time, particles will aggregate, and mass will be transferred from Class 1 to Class 2. This mass transfer can be estimated by

$$m_1(t) = \rho_p V_1 = m_{clay} - m_2(t) \qquad (25)$$

Where V_1 (L/L) represents the volume occupied by Class 1 particles per unit of volume. Most software's (LISST, Malvern ParticleSizer) give the relative % volume occupied by a class, which implies that V_1 can be evaluated from

$$V_1 = V_{1,\%} V_{tot} \qquad (26)$$

Where $V_{1,\%}$ is the volume occupied by Class 1 particles divided by the volume occupied by all particles. When the system is unflocculated, $V_{1,\%} = 1$ and one recover Eq. (24).

The mass transfer is represented in **Figure 7**. It is clear that the change in mass as function of time can be fitted using the same logistic growth functions used to fit the change in volume concentration (see **Figure 4**). These functions can subsequently be implemented in the numerical model, see Eqs. (10)–(12).

The density of Class 2 particles is evaluated according to Eq. (18). It is found that that between 500 s and 2000s the relative density of Class 2 flocs increases linearly from 30 to 36 g/L. As was already evident from the PSD analysis, the flocs have become denser over time, under the action of shear. After 24 h and being re-suspended, the relative density became about 140 g/L, which has to be compared with the mean value found by video microscopy, which is 340 g/L. There has been a significant increase in density overnight. The effect of deposition/resuspension is a topic that needs to be investigated further. From the estimation of the change in density and mean floc size over time, the settling velocity $w_{s,2}(t)$ (see Eq. (14)) can be estimated and implemented in the numerical model.

3.2 In-situ studies

3.2.1 Observed size, shape and behavior under flow

The large spread in particle size, aspect ratio and settling velocity found in laboratory experiments was also observed during in-situ video recordings, see **Figures 8** and **9**, performed during a 13 hours survey in the Rhine Region Of
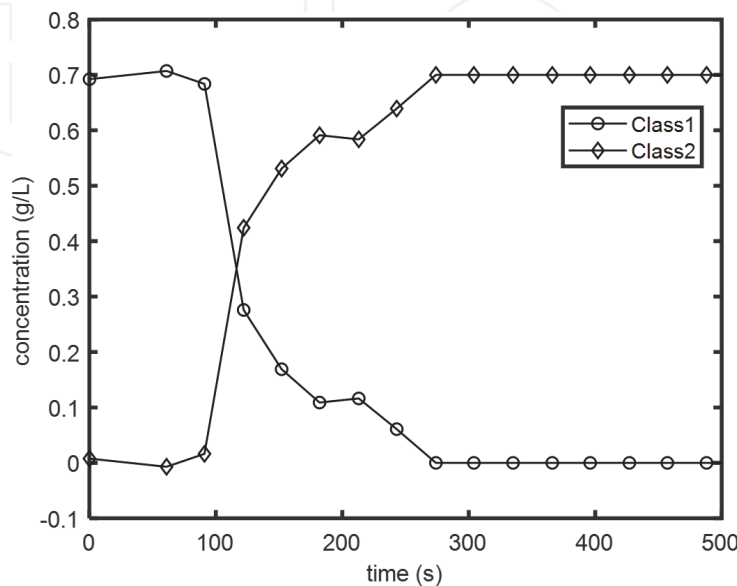

Figure 7.
Time evolution of the concentrations of mass classes 1 and 2 (given in the legends); clay suspension (0.7 g/L) in presence of 4.7 mg/L of cationic flocculant (added at t = 1 s).
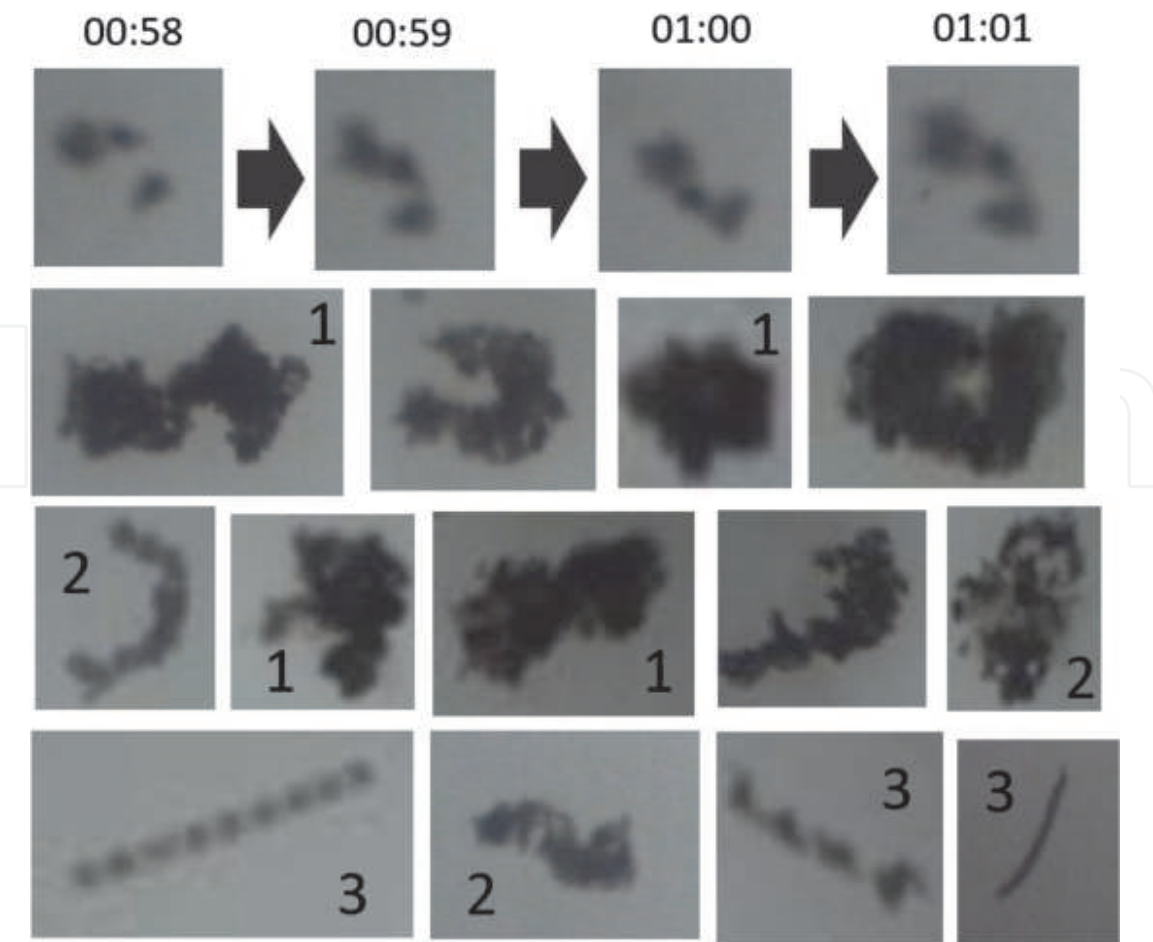
Figure 8.
Screenshots from the video recording taken with the underwater camera one meter above bed. Top panel: Aggregation of two flocs (video time indicated above the picture). The flocs stuck together at 00:59 and remained as one entity during the whole time they stayed in the field of view (until 01:02). Their shape adapted to the flow, indicating an elastic behavior (see 01:00 and 01:01). Some screenshots of typical flocs of largest size (100–500 μm) are given in the lower panels.
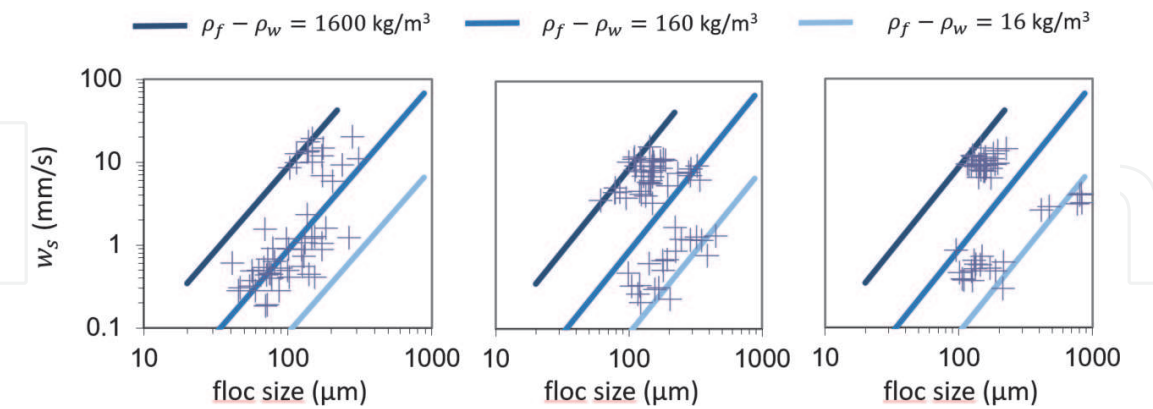

Figure 9.
Settling velocity distributions from LabsFLOC-2 measurements. From left to right, samples taken at: 06:00, 09:50 and 10:40 GMT. Data is adapted from [23].

Freshwater Influence (Rhine ROFI), about 10 km downstream of the mouth of the Rotterdam waterway, during a calm weather day, with low shear stresses and low SSC [32]. In **Figure 8** an illustration of in-situ flocculation is given: two flocs are observed to stick to each other and remain stuck in the hydrodynamic flow, displaying an elastic behavior. Flocs in situ are formed by aggregation of mineral sediment and both living and dead organic matter. Living organic matter is illustrated by the elongated particles in the lower panel which are formed by

aggregation of single algae cells. Some flocs are a combination of living cells, excreted polymers and mineral sediment.

Despite being measured during a calm day, the hydrodynamics at the measurement location are complex, owing to the regular passage of a fresh water front originating from the Rhine river. This results in the advection and diffusion of flocculated material close the bed, where the camera was positioned. The PSD was nonetheless relatively uniform over the whole day, and the number of particles per taken sample was low.

In **Figure 9** three settling velocities measurements performed on samples taken at different times of the day using the LabsFLOC-2 video microscopy technique are given. One can observe that particles have a large spread in size and settling velocities (and hence relative density).

By coupling the settling velocities results to the video microscopy observations, the density of particles can be estimated and three major types of flocs could be distinguished, based on their structure (indicated by a number in **Figure 8**).

1. compact flocs, containing a significant amount of mineral sediment, with an estimated density close to 2600 kg/m^3

2. flocs of various shape and structure, from elongated to coiled, in most of them strains of algae are still recognizable, with an estimated density close to 1160 kg/m^3.

3. bare algae strains, or strains coated with little amounts of debris, with an estimated density close to 1016 kg/m^3.

As was already found in laboratory experiments, density and floc size cannot be properly correlated: there is a wide spread in density in the [20–200] µm size class (Class 2a). As a lot of flocs of larger size are anisotropic, their equivalent diameter will have them part of the Class 2a (and not 2b). Moreover aspect ratio cannot be a proper variable to estimate settling velocities, as flocs are elastic and are prone to coil over time. In the next subsection, we will introduce a better variable to distinguish between different types of settling particles.

3.2.2 Variation with depth, tidal cycle and season

Many studies have confirmed the role of bio-cohesion in the formation of flocs [30, 33, 34]. In two recent studies, it was found that there is a correlation between flocculation and algal microorganisms presence in the water column, also outside the algae bloom season [35, 36]. This correlation can be studied using the sediment to algae concentration ratio, which is expressed as

$$ratio = \text{CC/SSC} \qquad (27)$$

where CC is the chlorophyll concentration (µg/L) and SSC the suspended sediment concentration (g/L). The data shown in **Figure 10** was collected in the South Passage of Changjiang Estuary (East China), for the summer period, when the amount of organic matter in the water column is significant [36]. A correlation was found between CC/SSC and particle density, evaluated from Eq. (18). The density was found to increase as function of CC/SSC in winter (when CC is constant over the whole water column), a low CC/SSC thus being associated with a high SSC. Particle density was found to decrease with CC/SSC in summer (when SSC is relatively constant over the whole water column), a low CC/SSC thus being
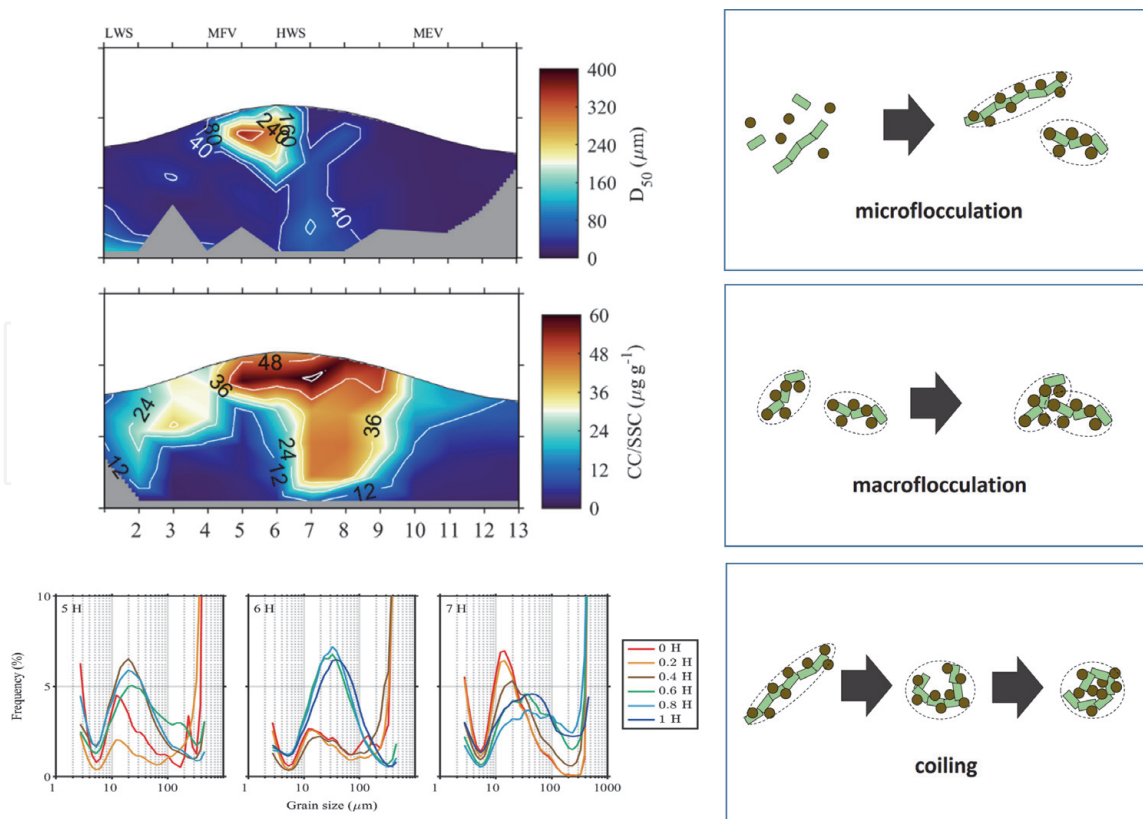
Figure 10.
Left panel: Recorded mean size (D50), estimated CC/SSC ratio and specific PSD's at different depths. Right panel: Schematic description of flocculation and re-sizing mechanisms happening in-situ. Data is taken from [28].

associated with a low CC. The D50 was found to be an exponentially decreasing function of particle density, in line with Eq. (22). Due the higher shear rates in summer, even silt particles could be entrapped in the flocs. These silt particles were even found at the top of the water column, as was assessed from laboratory PSD analysis on samples treated so as to remove organic matter.

The chlorophyll concentration (CC) was found to be relatively uniform over the whole water column in winter, with concentrations of about 0.6–1.0 µg/L. In summer the CC increased towards the bed with concentrations ranging from 1.3 to 3.7 µg/L. The CC/SSC ratio ranged from1.5 to 61.6 µg/L in summer, the higher values being found at the top of the water column, where algae activity is highest. A threshold value for CC/SSC was found to be 10–20 µg/L. Above the threshold value, flocs are predominantly governed by organic matter (algae), and bimodal PSD's are found, reflecting both the anisotropy of algae-containing flocs (known to lead to multimodal PSD peaks) along with their large spread in size. These flocs populate the whole water column in summer from the high water slack (HWS) period to ebb tide.

The PSD dynamics around HWS is particularly interesting and given in **Figure 10** as function of depth in the water column: 0H represents the surface water, whereas 1H represents the position just above bed. At 5 h, large particles are advected at the top of the water column from the seaside. At 6 h, two PSD's are observed. In the upper half of the water column [0H – 0.6H] the PSD peaks at about 20 µm (with a peak having an asymmetric shape towards the highest sizes – indicating the presence of large particles). In the lower half of the water column [0.6 – 1H] the PSD peaks at 30–50 µm and does not display any large PSD asymmetry. This transition seems to be in line with the change in salinity at HWS: algae-rich particles are trapped above the pycnocline, whereas clay-algae flocs are located

underneath. This trapping mechanism has been reported by several authors. During the period that algae-rich particles are trapped, microflocculation (the capture of fine mineral sediment by organic matter) can occur. As was seen from laboratory experiments, this flocculation is usually very fast, of the order of seconds or minutes. Due to the in-situ conditions (different mixing, lower SSC), the timescale for microflocculation could be slightly different, but is expected to be fast nonetheless.

Subsequently the algae-rich particles are slowly settling to the bottom of the water column, still capturing the finest fraction of mineral sediment that can be found at any depth in the water column. As the algae-sediment flocs are settling they can also experience macroflocculation (the capture of a floc by another one) and/or coiling. The CC/SSC ratio which is about 50 µg/g in the upper half of the water column increases from nearly 0 to 50 µg/g in the lower half as function of time. This implies that a significant amount of algae is reaching the seafloor. The particles residing below the pycnocline are denser, as they are composed of flocs with a large residence time in the water column (and hence are more prone to be coiled) and more susceptible to contain larger amounts of mineral sediment, since more mineral sediment is to be found at the bottom of the water column. During HWS both algae-rich and mineral-rich flocs settle down but do not necessarily catch-up (limiting macroflocculation), which explains the large polydispersity of the measured PSD's. It has similarly been found, by the analysis of different European estuaries [31], that the relative ratio of size class 2a (usually called "microflocs") and size class 2b (called "macroflocs") do not depend on shear and that the system composed of Class 2a flocs and Class 2b flocs is a steady-state – which is another indication that macroflocculation in the water column is not a major process.

4. Conclusions

In this chapter, the dynamics of flocculation are discussed in connection to both laboratory and in-situ experiments and observations. Three classes of particles, defined by mass, size and settling velocity have been presented and are summarized in **Table 2**.

The equation to be implemented in a sediment transport model relates to the process of "microflocculation" whereby mineral sediment of Class 1 is aggregating with organic matter, creating a Class 2a or Class 2b floc. The rate of mass transfer between Class 1 and Class 2 can be obtained from laboratory experiments in closed vessels (to ensure mineral mass conservation during the experiment), and linked with changes in particle sizes over time. Studying flocculation in closed vessels is at

Type	Mineral sediment (unflocculated)	Mineral sediment flocculated with organic matter	
Class	1	2a	2b
Size	< 20 µm	[20–200] µm	>200 µm
Mass transfer between classes	$m_1(t)$ (mass mineral sediment free in suspension)	$m_2(t)$ (mass mineral sediment inside flocs) $dm_2/dt = -dm_1/dt$	
Density and settling velocity	2.6 kg/L [0–0.5] mm/s	[2.6 − 1.16] kg/L [0.5–10] mm/s	[1.16 − 1.02] kg/L [0.5–10] mm/s

Table 2.
Definitions of the classes with associated size, mass concentration, density and settling velocity.

present done in conditions that differs from in-situ conditions. The shear stresses in particular are usually higher in laboratory experiments (to avoid settling of particles in pipes or jars), the mineral clay concentrations are higher than in-situ (to ensure a proper detection by laser diffraction) and differential settling/flocculation of flocs in high water columns, with finite residence time, ought to be better studied. More work is also required to link the settling velocities obtained from settling column experiments via Eq. (13) to estimated settling velocities from in-situ techniques using Eq. (18). The one example given in the chapter shows that the velocities were different even though of the same order of magnitude.

The process of "macroflocculation" whereby a Class 2a or Class 2b is aggregating with another Class 2a or Class 2b is found to be a minor process in the water column (but might play a significant role close to the bed, where flocs interact more). As microflocculation is fast it is expected that at the top of the water column, where large particles of organic matter (like algae) are advected in summer, Class 2b particles are predominantly formed. Class 2a particles can be formed in regions where organic matter is less abundant, or where the shear is high, as by shearing flocs become denser and get a more spherical shape (by coiling). Class 2b particles can thus become Class 2a particles over time, as was demonstrated by laboratory experiments, and visible from under-water video microscopy. Another source of Class 2a particles is originating from resuspension from the bed, as it was observed that upon resuspension flocs are denser and smaller than before deposition. More work is required to parametrize the boundary condition (deposition/erosion) at the bed and in particular the mass transfer between Class 2 and Class 1 in the bed. This boundary condition is of course crucial for any sediment transport model.

Acknowledgements

Author details

Claire Chassagne[1]*, Zeinab Safar[1], Zhirui Deng[1,2], Qing He[2]
and Andrew J. Manning[1,3,4,5]

1 Faculty of Civil Engineering and Geosciences, Department of Hydraulic
Engineering, Delft University of Technology, The Netherlands

2 State Key Laboratory of Estuarine and Coastal Research, East China Normal
University, Shanghai, People's Republic of China

3 Coasts and Oceans Group, HR Wallingford, Oxon, UK

4 Energy and Environment Institute, University of Hull, Hull, East Riding of
Yorkshire, UK

5 School of Biological and Marine Sciences, University of Plymouth, Plymouth,
Devon, UK

*Address all correspondence to: c.chassagne@tudelft.nl

IntechOpen

References

[1] Hesse, Roland F., Anna Zorndt, and Peter Fröhle. "Modelling dynamics of the estuarine turbidity maximum and local net deposition." Ocean Dynamics 69.4 (2019): 489-507.

[2] Grasso, Florent, et al. "Suspended sediment dynamics in the macrotidal Seine Estuary (France): 1. Numerical modeling of turbidity maximum dynamics." Journal of Geophysical Research: Oceans 123.1 (2018): 558-577.

[3] Le Normant, C. "Three-dimensional modelling of cohesive sediment transport in the Loire estuary." Hydrological processes 14.13 (2000): 2231-2243

[4] Blumberg, A.F., Z-G Ji, and C.K. Ziegler. 1996. Modeling outfall plume behavior using far field circulation model. Journal of Hydraulic Engineering. ASCE, Vol. 122, No. 11

[5] Van Maren, D. S., et al. "Formation of the Zeebrugge coastal turbidity maximum: The role of uncertainty in near-bed exchange processes." Marine Geology 425 (2020): 106186.

[6] Shen, X., Lee, B. J., Fettweis, M., & Toorman, E. A. (2018). A tri-modal flocculation model coupled with TELEMAC for estuarine muds both in the laboratory and in the field. Water research, 145, 473-486.

[7] Maggi, F. (2009). Biological flocculation of suspended particles in nutrient-rich aqueous ecosystems. Journal of Hydrology, 376(1-2), 116-125.

[8] Lai, H., Fang, H., Huang, L., He, G., & Reible, D. (2018). A review on sediment bioflocculation: Dynamics, influencing factors and modeling. Science of the total environment, 642, 1184-1200.

[9] Mietta, F., Chassagne, C., Verney, R., & Winterwerp, J. C. (2011). On the behavior of mud floc size distribution: model calibration and model behavior. Ocean Dynamics, 61(2-3), 257-271.

[10] Markussen, Thor Nygaard, and Thorbjørn Joest Andersen. "A simple method for calculating in situ floc settling velocities based on effective density functions." Marine Geology 344 (2013): 10-18.

[11] Smith, S. Jarrell, and Carl T. Friedrichs. "Image processing methods for in situ estimation of cohesive sediment floc size, settling velocity, and density." Limnology and Oceanography: Methods 13.5 (2015): 250-264.

[12] Manning, A. J., and K. R. Dyer. "A comparison of floc properties observed during neap and spring tidal conditions." Proceedings in Marine Science. Vol. 5. Elsevier, 2002. 233-250.

[13] Manning, Andrew J., Sarah J. Bass, and Keith R. Dyer. "Floc properties in the turbidity maximum of a mesotidal estuary during neap and spring tidal conditions." Marine Geology 235.1-4 (2006): 193-211.

[14] Manning, A.J., Whitehouse, R.J.S. and Uncles, R.J. (2017). Suspended particulate matter: the measurements of flocs. In: R.J. Uncles and S. Mitchell (Eds), ECSA practical handbooks on survey and analysis methods: Estuarine and coastal hydrography and sedimentology, Chapter 8, pp. 211-260, Pub. Cambridge University Press.

[15] Many, G., Bourrin, F., de Madron, X. D., Pairaud, I., Gangloff, A., Doxaran, D., ... & Jacquet, M. (2016). Particle assemblage characterization in the Rhone River ROFI. Journal of Marine Systems, 157, 39-51.

[16] Fettweis, Michael. "Uncertainty of excess density and settling velocity of mud flocs derived from in situ measurements." Estuarine,

Coastal and Shelf Science 78.2 (2008): 426-436.

[17] Russel, W. B., Russel, W. B., Saville, D. A., & Schowalter, W. R. (1991). Colloidal dispersions. Cambridge university press.

[18] Elimelech, M., Gregory, J., & Jia, X. (2013). Particle deposition and aggregation: measurement, modelling and simulation. Butterworth-Heinemann.

[19] Chassagne, C. (2020). Introduction to Colloid Science, Delft Academic Press, ISBN 9789065624376

[20] Chassagne, Claire, and Zeinab Safar. "Modelling flocculation: Towards an integration in large-scale sediment transport models." Marine Geology 430 (2020): 106361.

[21] Bubakova, P., Pivokonsky, M., and Filip, P. (2013). Effect of shear rate on aggregate size and structure in the process of aggregation and at steady state. Powder Technology, 235:540-549.

[22] P. Jarvis, B. Jefferson, J.Gregory, and S.A. Parsons. A review of floc strength and breakage. Water Research, 39:3121–3137, 2005.

[23] Manning, A. J., and K. R. Dyer. "A comparison of floc properties observed during neap and spring tidal conditions." Proceedings in Marine Science. Vol. 5. Elsevier, 2002. 233-250.

[24] Cahill, J., Cummins, P. G., Staples, E. J., & Thompson, L. (1987). Size distribution of aggregates in flocculating dispersions. Journal of colloid and interface science, 117(2), 406-414.

[25] Mietta, F. "Evolution of the floc size distribution of cohesive sediments", PhD thesis, Delft University (2010), ISBN 9789088911583

[26] Shakeel, Ahmad, Zeinab Safar, Maria Ibanez, Leon van Paassen, and Claire Chassagne. "Flocculation of clay suspensions by anionic and cationic polyelectrolytes: A systematic analysis." Minerals 10, no. 11 (2020): 999.

[27] Ibanez Sanz, M. E. Flocculation and consolidation of cohesive sediments under the influence of coagulant and flocculant. Diss. Delft University of Technology, 2018

[28] Manning, A. J., and K. R. Dyer. "Mass settling flux of fine sediments in Northern European estuaries: measurements and predictions." Marine Geology 245.1-4 (2007): 107-122.

[29] Dyer, K. R., and A. J. Manning. "Observation of the size, settling velocity and effective density of flocs, and their fractal dimensions." Journal of sea research 41.1-2 (1999): 87-95.

[30] Shen, X., Toorman, E.A., Lee, B.J., Fettweis, M., 2018b. Biophysical flocculation of suspended particulate matters in Belgian coastal zones. Journal of Hydrology 567, 238–252. https://doi.org/10.1016/j.jhydrol.2018.10.02

[31] Soulsby, R.L., Manning, A.J., Spearman, J., Whitehouse, R.J.S., 2013. Settling velocity and mass settling flux of flocculated estuarine sediments. Marine Geology 339, 1–12. https://doi.org/10.1016/j.margeo.2013.04.006

[32] Safar, Z. Suspended Particulate Matter formation and accumulation in the delta Diss. Delft University of Technology, 2021

[33] Maggi, F., Tang, F.H.M., 2015. Analysis of the effect of organic matter content on the architecture and sinking of sediment aggregates. Marine Geology 363, 102–111. https://doi.org/10.1016/j.margeo.2015.01.017

[34] Takabayashi, M., Lew, K., Johnson, A., Marchi, A., Dugdale, R., Wilkerson, F.P., 2006. The effect of nutrient availability and temperature on chain

length of the diatom, *Skeletonema costatum*. Journal of Plankton Research 28, 831–840. https://doi.org/10.1093/plankt/fbl018

[35] Deng, Zhirui, et al. "The role of algae in fine sediment flocculation: In-situ and laboratory measurements." Marine Geology 413 (2019): 71-84.

[36] Deng, Z., He, Q., Chassagne, C., & Wang, Z. B. (2021). Seasonal variation of floc population influenced by the presence of algae in the Changjiang (Yangtze River) Estuary. Marine Geology, 440, 106600